JACS
JOURNAL OF THE AMERICAN CHEMICAL SOCIETY
Article
pubs.acs.org/JACS

Redox Responsive Release of Hydrophobic Self-Healing Agents from Polyaniline Capsules

Li-Ping Lv,[†] Yi Zhao,[†] Nicole Vilbrandt,[‡] Markus Gallei,[‡] Ashokanand Vimalanandan,[§] Michael Rohwerder,[§] Katharina Landfester,[†] and Daniel Crespy*,[†]

[†]Max Planck Institute for Polymer Research, Ackermannweg 10, 55128 Mainz, Germany

[‡]Ernst-Berl Institute for Chemical Engineering and Macromolecular Science, Darmstadt University of Technology, Petersenstrasse 22, 64287 Darmstadt, Germany

[§]Max Planck Institute for Iron Research GmbH, Max-Planck-Strasse 1, 40237 Düsseldorf, Germany

Supporting Information

ABSTRACT: Redox-responsive nanocapsules consisting of conductive polyaniline and polypyrrole shells were successfully synthesized by using the interface of miniemulsion droplets as a template for oxidative polymerizations. The redox properties of the capsules were investigated by optical spectroscopies, electron microscopy, and cyclic voltammetry. Self-healing (SH) chemicals such as diglycidyl ether or dicarboxylic acid terminated polydimethylsiloxane (PDMS-DE or PDMS-DC) were encapsulated into the nanocapsules during the miniemulsion process and their redox-responsive release was monitored by ^{1}H NMR spectroscopy. The polyaniline capsules exhibited delayed release under oxidation and rapid release under reduction, which make them promising candidates for anticorrosion applications.

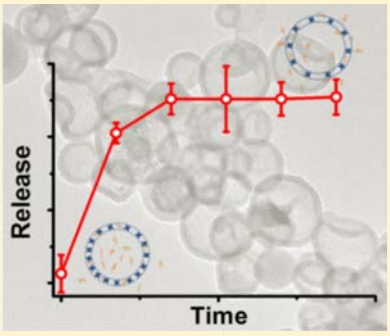

INTRODUCTION

Self-healing materials have gained considerable attention in recent years.[1] Among them, extrinsic SH materials play an important role in which healing agents were embedded into the materials in advance followed by the release and healing process when cracks occur. In most of the previous studies, the self-healing process is mainly triggered upon mechanical damage. However, a redox-responsive delivery of self-healing agents is also of large interest for certain applications such as for coatings for corrosion protection. Although the redox-stimulus was investigated as a trigger in intrinsic self-healing materials,[2] its use for the delivery of a hydrophobic self-healing agent is not yet reported. The introduction of redox-responsive units in materials allows a controlled change of interesting properties such as the permeability of the microcapsules shell,[3] the sol−gel transition of supramolecular gels,[2b] or chemical or drug-delivery upon redox trigger.[4] Among the manifold available polymers with redox properties,[5] conductive polymers are particularly interesting because of their high electrical conductivity and their good thermal and environmental stabilities.[6] The change in their conductivity, structure, color, volume, or hydrophilicity in response to electro- or chemical stimuli make them suitable for applications in drug delivery,[7] actuators,[8−10] memory devices,[11] light-emitting diodes,[12] or chemicals sensors.[13]

We show herein for the first time a release of hydrophobic chemicals triggered by a redox stimulus from capsules formed with conducting polymers. Polypyrrole (PPy)[14] and polyaniline (PANI)[15] are among the most investigated conducting polymers. Both of them have different possible oxidation states (Supporting Information Figure S1). For PANI, three oxidation states exist: the fully reduced leucoemeraldine (y = 1), the fully oxidized pernigraniline (y = 0), and the half-oxidized emeraldine (y = 0.5). Therefore, PPy and PANI can also exhibit redox-responsive properties upon electro- or chemical stimuli. PANI was also previously reported as an intelligent system for the release of corrosion inhibitors. The polymer could be reduced upon corrosion and the doping corrosion inhibitors could be released due to the galvanic coupling between corroded iron and polyaniline.[16] However, the poor solubility of PPy and PANI in ordinary organic solvents still hinders their applicability. To overcome the low solubility, PANI and PPy were processed in the form, for example, of nanocapsules by the thoroughly reported hard-template approach.[17] This approach however has intrinsic drawbacks. First, it is difficult to keep the structural integrity of such capsules, especially for thin capsules shells. Second, a further step is needed to encapsulate a substance inside the capsules. Besides, emulsions were also used as soft template to obtain hollow microspheres of polyaniline by using salicylic acid (∼1.5−3.1 μm in diameter) or β-naphthalene sulfonic acid (0.36−1.2 μm in diameter) as dopant.[18] Miniemulsion polymerization is known to be a versatile technique to prepare a wide range of polymers nanoparticles with various structures.[19] Because of the stability of the miniemulsion droplets,[20] the polymerization can be performed even in

Received: May 25, 2013
Published: August 20, 2013

   dx.doi.org/10.1021/ja405279t | J. Am. Chem. Soc. 2013, 135, 14198−14205

unconventional conditions such as in the absence of water in nonaqueous miniemulsions[21−23] and at high temperature.[23] Moreover, the miniemulsion process was already found to be useful for the encapsulation of self-healing agents in nanocontainers.[24] Aniline was already polymerized to yield monolithic particles in miniemulsion.[25] The release of water-soluble chemicals from microcapsules could be electrochemically controlled by the embedding of the microcaspules in polypyrrole films.[26] However, there is to the best of our knowledge no report about the release of hydrophobic chemicals controlled by the redox state of the polymer constituting the shell of nano- and microcapsules. Herein, we demonstrate a one-pot synthetic process for the formation of conducting polypyrrole and polyaniline capsules via miniemulsion polymerization. The interface of the miniemulsion droplets was used as soft template to perform the oxidative polymerization of aniline, allowing the encapsulation of a self-healing agent at the same time. The release behavior of the self-healing agent was studied as a function of the oxidation state of the formed polymer shells.

EXPERIMENTAL DETAILS

Materials. Aniline was purchased from Sigma Aldrich and distilled under vacuum before use. Pyrrole (Py, 99%), tetrahydrofuran (THF, ≥99.9%), ethylbenzene (EB, 99.8%), hexadecane (HD, 99%), methyl methacrylate (MMA, 99%), butyl acrylate (BA, >99%) and ammonium persulfate (APS, 98%) were obtained from ACROS Organics and used as received. Sodium dodecyl sulfate (SDS, 99%), poly(dimethylsiloxane) diglycidyl ether terminated (PDMS-DE, $M_n \approx 800$ g mol^{-1}), pyrene (>99%), hydrazine aqueous solution (N_2H_4, 35 wt % in H_2O), potassium persulfate (KPS, ≥99%), and hydrogen peroxide solution (H_2O_2, 34.5−36.5%) were supplied from Sigma Aldrich and used as received. Poly(vinyl alcohol) (PVA, Alfa Aesar, 98−99% hydrolyzed) with a molecular weight M_w of 27450 g mol^{-1} (measured by gel permeation chromatography, calibration with poly(ethylene oxide) (PEO) standards, 80% 0.1 M $NaNO_3$ in water/20% MeOH as eluent), polydimethylsiloxane carboxydecyldimethyl terminated (PDMS-DC, ABCR, $M_w \approx 1000$ g mol^{-1}), Lutensol AT50 (BASF), poly(vinyl alcohol) (PVA, Polysciences Inc., $M_w \approx 25\,000$ g mol^{-1}, 88 mol % hydrolyzed) were used as received.

Formation of PANI Nanocapsules. PANI capsules were prepared as follows: a mixture of aniline (0.49 mL, 5.38 mmol) and ethylbenzene (1.23 mL, 10.04 mmol) as hydrophobe was added to 6 mL of water containing 62.5 mg of SDS. After stirring under 1000 rpm for 1 h at room temperature, the emulsification was carried out by ultrasonicating the mixture for 240 s at 90% amplitude (Branson sonifier W450) under ice cooling. After emulsification, an aqueous solution of PVA (10 wt %) was mixed with the miniemulsion. Then, an aqueous solution of APS (1.23 g, 5.38 mmol in 1.67 mL of water) was added dropwise to the miniemulsion at room temperature. The color of the miniemulsion first turned brown then dark green as the polymerization proceeded. This sample was defined as PANI-1. The other PANI sample was obtained by increasing the concentration of monomer in the dispersed phase and was defined as PANI-2. The encapsulation process of self-healing agents was carried out during the formation of PANI capsules. PDMS-DE or PDMS-DC (60 wt % compared to monomer) was dissolved in the dispersed phase prior to the emulsification. The samples were defined as PANI/PDMS-DE and PANI/PDMS-DC, respectively.

To calculate the encapsulation efficiency, 102.5 mg of PANI/PDMS-DC or PANI/PDMS-DE capsules dispersions were first freeze-dried and then dissolved in a mixture of 1 mL of NMP and 1 mL of DMSO for 24 h. 0.4 mL of the solution was taken for ^{1}H NMR measurement in 0.7 mL of THF-d_8 with pyrene as internal standard. In parallel, same amounts of PANI/PDMS-DC or PANI/PDMS-DE capsules dispersions were purified by centrifugation in water. The collected capsules were then prepared by the aforementioned method for ^{1}H NMR spectroscopy. The encapsulation efficiency of PDMS-DC in PANI capsules was obtained by comparing the signals of −Si-CH_3 from PDMS-DC around 0 ppm in ^{1}H NMR before and after purification. The encapsulation efficiencies for the PANI/PDMS-DE and PDMS-DC systems were found to be ∼94% and ∼89%, respectively.

Formation of PPy Nanocapsules. PPy nanocapsules were prepared using a similar process with PANI capsules. The difference is that hexadecane was added in the dispersed phase, that is, EB/HD (2/3, V/V), a higher ratio continuous/dispersed phase (95/5, V/V) was adopted, and that the polymerization was carried out at 0 °C.

Redox-Responsive Properties of PANI Capsules. Before the addition of oxidizing or reducing agents, the dispersions of PANI capsules were purified by centrifugation to remove PVA until a clear supernatant was observed. Certain amounts of PANI capsules dispersions were taken and added in hydrogen peroxide or hydrazine solution with a molar ratio ANI unit to N_2H_4 or H_2O_2 equal to 1:43. After reaction and stirring for 12 h, an aliquot of the dispersion was taken for electron microscopy measurements. The rest of the sample was freeze-dried for further FT-IR, UV−vis measurements.

Redox-Responsive Release of Self-Healing Agents from PANI Capsules. The redox release behavior of PANI capsules were detected as follows: the miniemulsion dispersion of PANI capsules after polymerization was first mixed with same weight of distilled water to lower the initial concentration. After that, several 5 mL glass vials were separately added in 102.5 mg of these diluted PANI capsules dispersion. Then 0.7 mL of deuterated tetrahydrofuran (THF-d_8) which dissolved certain amount of pyrene before use, together with 74 μL of N_2H_4 or H_2O_2 solution (molar ratio ANI unit to N_2H_4 or H_2O_2 1:43) were added. As a control, the same amount of distilled water was used instead of a N_2H_4 or H_2O_2 solution. After stirring for different times, the mixture was kept till phase separation occurred and the supernatant was taken for ^{1}H NMR measurements.

The release of PDMS-DE or PDMS-DC was detected by comparing the separated signal of −Si-CH_3 from PDMS-DE around $\delta \approx 0$ ppm with the signal of pyrene around $\delta \approx 8$−8.5 ppm after different times. To detect the total amount of self-healing agents inside of the release samples, same amount of diluted capsules dispersion was first freeze-dried and then dissolved in the mixture of 1 mL of DMSO and 1 mL of NMP under stirring for 12 h. Then 0.2 mL of the mixture was taken and added in 0.7 mL of THF-d_8/pyrene solution.

In the case of the sample that was first oxidized then reduced after 24 h of release, fresh hydrazine solution with the amount of twice as much as the initial amount of hydrogen peroxide solution was added into the oxidized sample after 24 h of release.

Analytical Methods. The FTIR spectra of polymers were measured on KBr pellets using a Perkin-Elmer spectrum BX FT-IR spectrometer. All spectra were collected in the range of 400−4000 cm^{-1} with a resolution of 1 cm^{-1}. Freeze-dried PANI capsules were dissolved in *N*-methyl-2-pyrrolidone (NMP) for UV−vis measurements recorded with a Perkin-Elmer Lambda 25 UV−vis spectrometer. The morphology of the capsules were examined with a Gemini 1530 (Carl Zeiss AG, Oberkochem, Germany) scanning electron microscope (SEM) operating at 0.2 kV. Samples for SEM were prepared by dropping purified capsule dispersions on silicon wafers and were dried at room temperature. The morphology of the capsules was also studied using a transmission electron microscope (TEM) (Zeiss EM912) operating at an accelerating voltage of 120 kV. All samples were deposited on a 300 mesh carbon-coated copper grid. Atomic force microscope (AFM) measurements were carried on a commercial Bruker Dimension 3100 (NanoScope IIIa controller) setup in tapping mode. Hydrodynamic diameters (D_h) of the capsules (dispersions diluted in 3 mg mL^{-1} of SDS aqueous solution) were determined with a dynamic light scattering (DLS) device (NICOMP 380, Santa Barbara) at a fixed angle of 90° and a laser diode running at 635 nm. Energy-dispersive X-ray spectroscopy (EDX) measurement was carried on a scanning electron microscope (Hitachi SU8000) combined with a Bruker Axs XFlash 5010 under 5 kV. ^{1}H NMR spectra were measured at room temperature on a console Avance 300. The partition coefficient of the monomers aniline and pyrrole in the

dx.doi.org/10.1021/ja405279t | J. Am. Chem. Soc. 2013, 135, 14198−14205

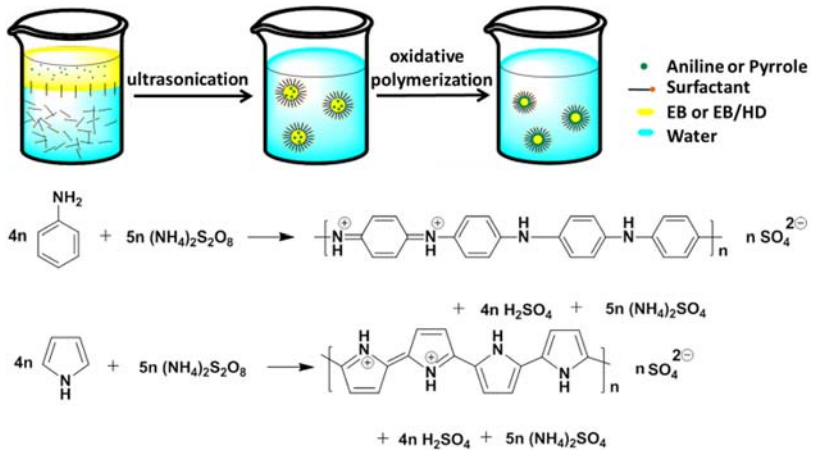

Figure 1. Oxidative polymerization of aniline or pyrrole in miniemulsion to form conductive polymer nanocapsules in the presence of ethylbenzene (EB) or ethylbenzene/hexadecane (EB/HD).

dispersed and continuous phases was estimated by mixing the two phases (same quantities as for the miniemulsions) but without surfactant and initiator. After stirring, the two phases were separated, isolated, and aliquots were taken to be dissolved in DMSO-d_6.

The partition coefficient f_M of the monomer was then calculated with the following equation:

$$f_M = \frac{c_M(d\varphi)}{c_M(c\varphi)}$$

with $c_{M(d\varphi)}$ and $c_{M(c\varphi)}$ being the concentrations of monomer in the dispersed and continuous phase, respectively.

The apparent molecular weight of the polymer samples were measured by gel permeation chromatography (GPC) using *N*-methyl-2-pyrrolidone (NMP)/LiBr as eluent. Calorimetric measurements of aniline polymerization were performed in a μRC microreaction calorimeter (C3 Prozess- and Analysentechnik GmbH, Germany). After the preparation of aniline miniemulsions as described previously, 1 mL of the miniemulsions and a stir bar were added into a small vial without adding the initiator; 200 μL of molten octadecane was added above the miniemulsion heated at 40 °C and left to solidify at room temperature to form a thin film. After that, a drop of an APS aqueous solution (equimolar amount compared to the monomers) was added on the octadecane solid film. Then the vial was placed inside the sample cell of the calorimeter. The sample was left to equilibrate and the measurement was started by using a needle to break the film between the miniemulsion and the initiator solution. The heat flux generated during the polymerization of aniline was measured in function of the reaction time. Calorimetric measurements of the aniline polymerization in DMSO were conducted with the same method. Water was also used to replace APS aqueous solution to perform a control experiment. CV measurements were carried out with a multipotentiostat VMP2 (Princeton Applied Research) with a custom-made cell. PANI capsules dispersed in water (10 mg mL^{-1}) were drop-casted on an ITO slide.[36] The sample was dried overnight at room temperature and directly used for CV measurements. CV was measured under nitrogen in aqueous HCl (1 M) as electrolyte. Ag/AgCl reference electrode and Pt counter electrode were chosen and measurements were carried out with a scan rate of 50 mV s^{-1} in a range of −0.4 to 1.2 V. The PPy capsules dispersed in water (10 mg mL^{-1}) were deposited on a glassy carbon electrode.[37] The electrode was dried overnight at room temperature and directly used for CV measurements. CV was measured under nitrogen atmosphere in 0.1 M aqueous phosphate buffered saline as electrolyte. Ag/AgCl reference electrode and Pt counter electrode were chosen with and measurements were carried out with a scan rate of 100 mV s^{-1} in a range of −0.2 to 1.0 V. All potentials refer to Ag/AgCl reference electrodes.

RESULTS AND DISCUSSION

Formation of the Nanocapsules. Oxidative polymerization of aniline and pyrrole was conducted in direct miniemulsion to form PANI and PPy nanocapsules, respectively. In the initial stage, there were two separated phases: the continuous phase composed of the aqueous solution of surfactant, and the dispersed phase containing the monomer and the nonpolar solvents. After mixing and ultrasonication, the miniemulsion dispersion was formed in which droplets containing some monomer and the nonpolar solvents were stabilized by the surfactant (see Figure 1).

The droplet interface between the aqueous phase and the oil phase was used as template for the precipitation of the growing polymer chains. The partition coefficient f_{ANI} was estimated to be equal to 11 as determined by ^{1}H NMR, that is, ∼92% of the ANI was present in the dispersed phase. Thus, as the aqueous solution of oxidant was added to the miniemulsion, APS molecules reacted with the ANI in the continuous phase and the growing chain nucleated the miniemulsion droplets (see Supporting Information Figure S2a). The polymer chains precipitated after a critical degree of polymerization on the interface of the droplets, because of the poor solubility of the polymer in water and in the (anti)solvent present in the dispersed phase, mainly from the inside of the droplets. The kinetics of the reaction was followed by calorimetry and revealed two interesting informations. First of all, the reaction took less than 30 min to be completed with most of the heat generated in the first 3 min. Second, the profile displayed two peaks whereas only one peak was observed in a polymerization of ANI in DMSO prepared for comparison (Supporting Information Figure S3a,b). One probable explanation for this difference is the partition of the monomer in the two liquid phases. It is important to note that the samples were not completely thermally equilibrated because of stability issue of the miniemulsions relative to the reaction speed and therefore the classical setup was modified accordingly (see Supporting Information for details). The case of Py is unconventional because the partition coefficient f_{Py} was estimated to be 0.8, that is, a significant amount of the monomer (∼55%) was in the continuous phase. Thus, the growing chains of polypyrrole probably precipitated both from the inside and the outside of the miniemulsion droplets. A scheme displaying both scenarios (for ANI and Py) is depicted in Supporting Information Figure S2. The heat flux generated during the polymerization of

dx.doi.org/10.1021/ja405279t | J. Am. Chem. Soc. 2013, 135, 14198−14205

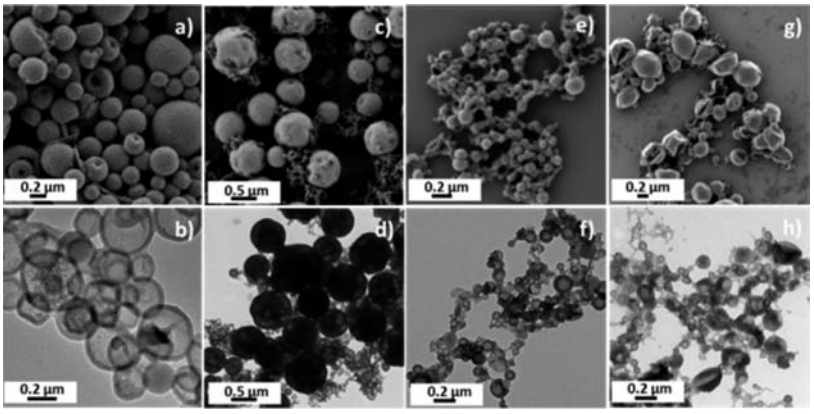

Figure 2. SEM and TEM micrographs of the PANI with (a–b) lower fraction of monomer (PANI-1), (c–d) higher fraction of monomer (PANI-2). PPy capsules with (e–f) lower fraction of monomer (PPy-1), (g–h) higher fraction of monomer (PPy-2).

Table 1. Summary of Characteristics of PANI and PPy Dispersions

polymer	M[a]/EB/HD [v/v/v]	conversion[b] [%]	M_w[c] [g mol^{-1}]	d[d] [nm]	morphology[d]
PANI-1	29/71/0	72	20050	720 ± 530	hollow sphere
PANI-2	95/5/0	79	10950	690 ± 322	multihollow sphere
PPy-1	30/28/42	66	n.a.	80 ± 50	hollow sphere
PPy-2	20/32/48	71	n.a.	110 ± 70	hollow sphere

[a]*M* = aniline or pyrrole. [b]Calculated from ^{1}H NMR spectroscopy. [c]Obtained from GPC. [d]Determined from 100 particles by electron microscopy.

pyrrole in miniemulsion displayed only one peak whereas the polymerization of ANI displayed two peaks. This is probably explained by the faster polymerization kinetics of Py.

After the polymerization, PANI or PPy nanocapsules filled with EB or EB/HD are detected. It has been reported previously that the addition of a second stabilizer after the emulsification,[25a] for example, polyvinylalcohol (PVA) or polyvinylpyrrolidone (PVP), was necessary to stabilize the polymer particles because of the high ionic strength of the dispersions. The increase of viscosity due to the addition of the stabilizer in the continuous phase allows for lowering the rate of coalescence since the droplets diffuse more slowly. The polymerization of aniline without additional stabilizer (PVA or PVP) for the synthesis of capsules did not result in stable dispersions.

The morphology of PANI (Figure 2a–d) and PPy (Figure 2e–h) particles was observed by electron microscopy. For PANI, different morphologies were formed while increasing the ratio of ANI: EB. PANI with lower monomer concentration (PANI-1) appeared as hollow spheres with thin shells as determined by TEM (Figure 2b). Particles prepared with a higher amount of monomer (PANI-2) exhibited a multihollow morphology and kept their structural integrity even under the high vacuum of SEM (Figure 2c). The formation of particle structures with multiple domains inside is kinetically controlled and can be achieved owing to the high concentration of monomer in the droplet and because the polymerization reaction is very fast. The small amount of solvent and remaining nonreacted monomer is dispersed in the PANI particles after the polymerization and form multihollow structure after evaporation. The average diameters of these PANI capsules are 720 and 690 nm (Table 1). The relatively large size and distribution of size is a clear indication that the miniemulsions were destabilized during the polymerization reaction due to the high ionic strength in the dispersion. We also found that below the feed ratio of monomer in the dispersed phase, the type of surfactant and additional stabilizer (PVA or PVP) exhibited effects on the colloidal morphology. For example, when PVP K30 was employed instead of PVA, aggregates of nanoparticles were formed (Supporting Information Figure S4a) which indicated that PVP K30 is not an efficient stabilizer in our system. Changing the ionic surfactant SDS to the nonionic Lutensol AT50 and using PVP K30 as additional stabilizer led to the formation of microrods (Supporting Information Figure S4b). In order to slow down the reaction and the coalescence, ANI was polymerized in heterophase slightly above 0 °C. Compared to the synthesis performed at room temperature, the color change of the miniemulsion took longer time as polymerization proceeded, which indicated a slower reaction. However, the colloidal morphology of PANI was found to be the same as shown in Supporting Information Figure S5.

The structure of PPy nanocapsules synthesized with distinct monomer concentration is shown in Figure 2e–h. In both cases (Table 1), well-defined core–shell morphologies were obtained. Increasing the monomer concentration to 96% however yielded aggregates of homogeneous nanoparticles (PPy-3, Supporting Information Figure S6). The PPy colloids were much smaller than the PANI colloids prepared under similar conditions. This can be explained by the presence of hexadecane (HD) in the dispersed phase of the Py miniemulsions, which is much less soluble in water than ethylbenzene (EB) and therefore is more efficient to hinder Ostwald ripening of the miniemulsions. Besides, the formation of PPy particles was also varied under different reaction temperatures. As shown in Supporting Information Figure S7, PPy nanocapsules formed at room temperature exhibit a higher size distribution than those formed at 0 °C. This can be attributed to the increase of coalescence rate with temperature. It should be noted that, in the synthesis of PPy nanocapsules, the nonsolvent for the polymer was a mixture of EB and HD, differently from the case of the ANI polymerization where only

dx.doi.org/10.1021/ja405279t | J. Am. Chem. Soc. 2013, 135, 14198–14205

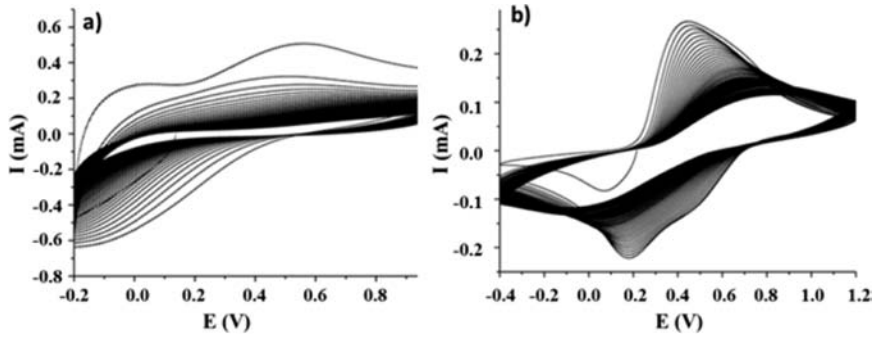

Figure 3. Cyclic voltammograms of (a) PPy and (b) PANI. Measurements were carried out over 60−80 reduction/oxidation cycles with applied scan rates of 100 mV s^{-1} (PPy) and 50 mV s^{-1} (PANI).

EB was used. In the case of aniline, capsules were easily formed by using the sole EB as hydrophobe, whereas only nanoparticles were generated under the same conditions for pyrrole polymerization (Supporting Information Figure S8). This observation can be explained by considering the solvent quality of EB and HD for the polymers, and the fact that the oxidation of pyrrole is faster than for aniline.[27] The latter fact induces that the PPy chains precipitated too fast to be able to diffuse to the interface of the droplets. Shifting the composition of the solvent toward a lower quality changes the partition of the monomer in the dispersed phase and continuous phases as shown above. In the case of Py and for droplets containing a high amount of HD, the PPy chains can precipitate from the continuous phase to the droplets interfaces.

The reactive efficiency of aniline and pyrrole in miniemulsion polymerization was determined by the conversion of monomer as shown in Table 1. The calculation of conversion was obtained by comparing the signal of aniline or pyrrole in ^{1}H NMR spectra before and after the polymerization reaction (Supporting Information Figure S9). For these measurements, the nonpolar solvent, EB, was used as internal standard. As shown in Table 1, PANI-1 and -2 had 72 and 79% of converted monomer while for PPy-1 and PPy-2, the conversion was 66 and 71%, respectively. An even higher monomer conversion (>99%) was also obtained in the case of pyrrole when only EB was used in the dispersed phase.

Redox-Responsive Properties of PANI Capsules. To study the redox-response and the reversibility of the oxidation/reduction process, cyclic voltammetry measurements were carried out both for PPy-1 and PANI/PDMS-DE capsules. In the case of PPy capsules, the capsules dispersed in water were dropped on a glassy carbon electrode followed by drying of the electrodes overnight at room temperature. CV measurements were carried out with 60 cycles in 0.1 M phosphate buffered saline solution revealing a significant loss of signal intensity after the first cycle (Figure 3a). In the case of PANI capsules the stable capsules water dispersion was dropped on an ITO slide followed by drying of the sample overnight. Notably, even after 80 reduction/cycles in 1 M aqueous hydrochloric acid, remarkable signal intensity could be obtained in cyclic voltammograms (Figure 3b). Therefore, PANI was selected for further investigations of the redox-responsive properties of the capsules.

The redox-responsive properties of PANI capsules were studied by optical spectroscopy and electron microscopy. Previous study showed that the oxidation degree of PANI can be estimated by comparing the intensity of quinonoid and benzenoid peak appearing in IR spectra. The degree of oxidation x was calculated from the intensity of the quinonoid peak I_Q relative to the benzenoid peak I_B,[28,29] using the equation:

$$x = \frac{I_Q}{I_Q + I_B}$$

Thus, the oxidation degree of the fully reduced polyaniline is estimated to 0 and the fully oxidized polyaniline to 50%. The chemical structures of PANI before and after oxidizing or reducing were characterized by FT-IR as shown in Supporting Information Figure S10. Absorption peaks around 1138, 1295, 1497, and 1578 cm^{-1} were attributed to the C═N stretching, C−N stretching, and stretching vibrations of the benzenoid and quinonoid rings, respectively. According to the above equation, the oxidation degree of PANI-1 and PANI-2 was calculated to be 45.1% and 44.6%, respectively. As for PANI-1, the oxidation degree (44.4%) did not vary much after oxidation by H_2O_2 after 12 h. After the reduction of PANI-1 by N_2H_4, the oxidation degree was estimated to 37.9%, which means that the oxidation degree was decreased by ∼16% compared to the nonreduced PANI (45.1%). The quinonoid peak sharply decreased compare to benzenoid peak upon reduction (Supporting Information Figure S10a, red line). These observations were confirmed by UV−vis spectroscopy (Supporting Information Figure S10b). The peaks around 600 nm were assigned to the excitonic transition between the highest occupied molecular orbital (HOMO) of the bezenoid ring (nonbonding nitrogen lone pair) and the lowest unoccupied molecular orbital (LUMO) of the quinonoid ring.[30−31] The absorption peak around 600 nm exhibits a blue-shift when PANI is oxidized and disappears upon reduction.[32] In our case, the PANI after oxidation did not exhibited much change, i.e. the maximum absorption changed from 571 to 567 nm after oxidation (Supporting Information Figure S10b), but the reduced PANI showed a pronounced intensity decrease (∼ 42%) due to the lower oxidation degree after reduction. The change of color could be visually evidenced (Supporting Information Figure S11), especially after reduction of the PANI. The morphology of the capsules after reduction and oxidation was observed by electron microscopy. After oxidation, the morphology of PANI capsules (Supporting Information Figure S12a,b) was similar to the initial PANI-1 capsules (Figure 1a,b). However, the reduced PANI sample exhibited many collapsed capsules (Supporting Information Figure S12c,d). This is also an indirect indication that the reduction of the PANI was successful because it is known that reduced PANI possesses a decreased rigidity.[33]

dx.doi.org/10.1021/ja405279t | J. Am. Chem. Soc. 2013, 135, 14198−14205

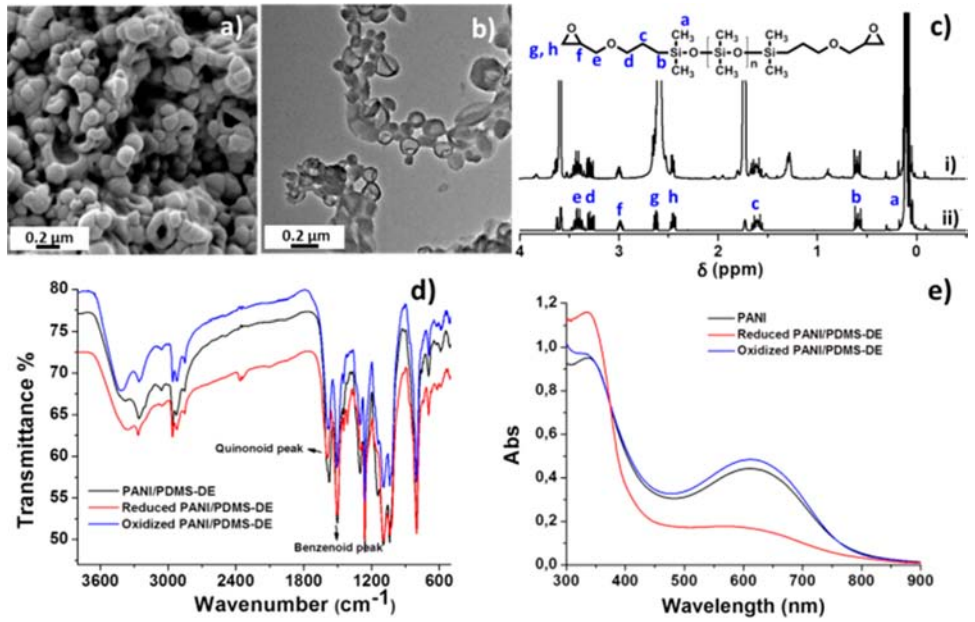

Figure 4. (a) SEM and (b) TEM micrographs of PANI/PDMS-DE capsules after purification; (c) ^{1}H NMR of PANI/PDMS-DE (i) capsules after purification, drying, grinding and dissolution of the PDMS-DE in $CDCl_3$ and pure PDMS-DE (ii). (d) FT-IR and (e) UV−vis spectra of purified PANI/PDMS-DE before and after reduced or oxidized by N_2H_4 or H_2O_2 aqueous solution for 12 h. The molar ratio of ANI unit to N_2H_4 or H_2O_2 was set as 1:43.

Redox-Responsive Release of Self-Healing Agents from PANI Capsules. The redox-responsive properties of the PANI capsules were further investigated for the selective delivery of chemicals. We selected polydimethylsiloxane diepoxide- or dicarboxylic acid-terminated (PDMS-DE or PDMS-DC) as healing agents[24e] for a self-healing reaction based on polycondensations. The PDMS-DE was successfully encapsulated (~94% encapsulation efficiency) in the PANI nanocontainers as shown by electron microscopy (Figure 4a-b) and was intact as verified by ^{1}H NMR spectroscopy (Figure 4c). Larger PANI/PDMS-DC capsules could be also prepared with a thicker shell of 56 ± 7 nm (Supporting Information Figure S13).

The distinct sharp absorption peaks around 800 and 1260 cm^{-1} in Figure 4d could be attributed to the Si-CH_3 group from PDMS-DE in purified PANI capsules containing PDMS-DE. Once again, only minor changes occurred in oxidized samples. The oxidation degrees calculated from the FT-IR spectra changed from 44.5% to 43.8% and decreased to 39.5% after reduction. The UV−vis absorption maxima exhibited a very minor blue-shift (612 to 610 nm) after oxidation and a large decrease of intensity (~62%) after reduction. The same trends were observed for the morphologies of the PANI/PDMS-DE capsules after oxidation or reduction, that is, the morphology after oxidation remained similar to the untreated caspules whereas the structures of the reduced capsules were collapsed and film formation due to the release of PDMS-DE could be detected (Supporting Information Figure S14).

The redox-responsive release of PDMS-DE was monitored by ^{1}H NMR spectroscopy by comparing the chemical shift of released PDMS-DE at 0 ppm to the one of pyrene at 8.5 ppm taken as internal standard. The release curves shown in Figure 5 demonstrated three different behaviors depending on the nature of the added solution (reductant, oxidant, or water). The reduced sample exhibited a fast release of PDMS-DE in the first 30 min, which is corroborated by the quick color change after

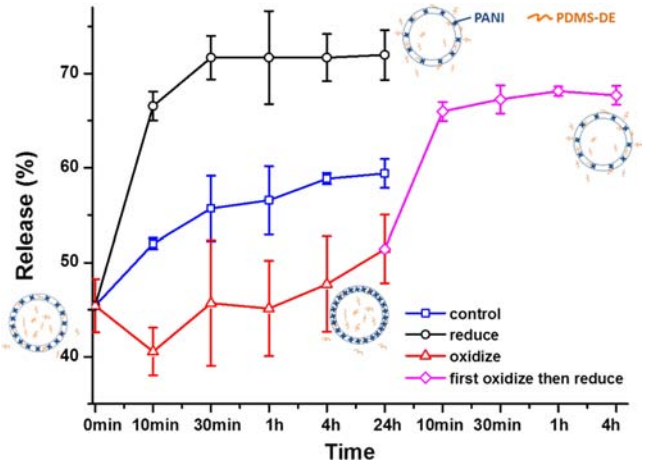

Figure 5. Release of PDMS-DE from PANI capsules under different condition. In the control experiment, the same volume of solvent and reactants are used but without oxidizing or reducing agents.

addition of the reductant. The control sample (addition of water) showed also a release of PDMS-DE because of the diffusion of PDMS-DE in THF. The addition of the oxidant caused a slower release behavior, even compared to control sample. After addition of an excess of the reductant to the previously oxidized capsules, the release stimulated by reduction was again observed. A similar behavior was observed for the PANI/PDMS-DC capsules (Supporting Information Figure S15). A notable difference was the amount of nonselective release at t = 0 that was lower (~28%) than for the PANI/PDMS-DE capsules explained by the thicker shell of PANI/PDMS-DC capsules. When the capsules are purified prior to the release experiment to remove the nonencapsulated PDMS, the nonselective release at t = 0 dropped to ~13%. The release properties of the capsules can be therefore optimized by

dx.doi.org/10.1021/ja405279t | J. Am. Chem. Soc. 2013, 135, 14198−14205

increasing the shell thickness and by removing the non-encapsulated self-healing agents prior to their uses.

Upon oxidation of the PANI, some benzenoid rings will be partly oxidized to quinonoid rings, leading to amine-imine intermolecular hydrogen bonding.[34] The polymer chains are then more compact and hinder the release process. In the case of the reduced sample, several factors play a role. First, the hydrogen bonding becomes weaker and polymer chains therefore looser in the capsule membrane. Second, the presence of more rotatable single bonds in reduced PANI decreases the rigidity of the PANI chains and increases their mobility. Third, it is known that PANI exhibits different permeability and wettability depending on the redox and doping state.[35] For example, more water permeability was found for doped PANI films than undoped (reduced) films due to the increase of hydrophilicity in the oxidized state.[35] The release of PDMS-DE from PANI capsules under reduction is therefore promoted by the presence of more flexible PANI chains and the decreased hydrophilicity of the membrane facilitating the permeability of the hydrophobic PDMS-DE.

Finally, the capsules were embedded either in a hydrophilic PVA film or in a hydrophobic acrylate coating since there were already investigated as passivation layers for anticorrosion.[38] The PVA containing capsules was redissolved in water to extract the capsules that were isolated and analyzed by atomic force microscopy (AFM) and gravimetry (Supporting Information). The morphology of the capsules before and after embedding exhibited only minor differences (Supporting Information Figure S16). Indeed, less than 5% of the observed capsules were found to have a collapsed structure after their extraction from the PVA. The determination of the amount of PDMS-DC in the extracted capsules by ^{1}H NMR spectroscopy measurements revealed that only a minor amount (∼1%) of PDMS-DC was leaking from the inner core of the capsules (see Supporting Information for the details). However, it was not possible to extract selectively the capsules from the hydrophobic acrylate coatings. However, SEM images of the cross-section of acrylate coatings (Supporting Information Figure S17) showed that the capsule structure remained intact after being embedded in the acrylate coatings. The comparison between EDX spectra taken on the acrylate matrix and on a capsule embedded in the acrylate coating reveals that the presence of silicon in the latter location (Supporting Information Figure S18). Because the PDMS-DC is the only possible source of silicon in the system, the results indicates that PDMS-DC remained encapsulated in the PANI containers that are embedded in the acrylate coatings. The capsules/acrylate coating could be also prepared on a zinc foil (Supporting Information Figure S19). Silicon from PDMS-DC could not be detected from EDX measurements performed on the matrix of the capsules/acrylate coating whereas a clear signal for silicon was detectable at the location of the capsules (Supporting Information Figure S20). The PDMS-DC self-healing agent could therefore be kept inside the capsules after being embedded in the hydrophobic acrylate coating.

■ CONCLUSIONS

Polypyrrole (PPy) and polyaniline (PANI) capsules were synthesized by oxidative polymerization using miniemulsion droplets as soft templates. The chemical structure and morphology of the PANI capsules was controlled by varying their oxidation states as shown by a combination of FT-IR and UV−vis spectroscopy, electron microscopy, and cyclic voltammetry measurements. A hydrophobic liquid self-healing agent was successfully encapsulated in the PANI capsules and its redox-responsive release was monitored by ^{1}H NMR spectroscopy. The release could be stimulated upon reduction and delayed under oxidation. Since the PANI polymer was already applied for anticorrosion,[16] the PANI containers with encapsulated self-healing agent are promising candidates for anticorrosion and self-healing applications in metallic systems.

■ ASSOCIATED CONTENT

Supporting Information

Oxidation states of polyaniline, schematics for the capsules formation, calorimetric thermograms, electron microscopy micrographs of the capsules, NMR, IR and UV spectra, photographs of the polyaniline solution with different oxidation states, redox-responsive release of PDMS-DC from the capsules, AFM and SEM-EDX measurements on capsules embedded in the coatings. This material is available free of charge via the Internet at http://pubs.acs.org.

■ AUTHOR INFORMATION

Corresponding Author

crespy@mpip-mainz.mpg.de

Notes

The authors declare no competing financial interest.

■ ACKNOWLEDGMENTS

D.C. and M.R. gratefully acknowledge financial support from the DFG (SPP1568 "Design and Generic Principles of Self-Healing Materials"). M.G. thanks the Landesoffensive zur Entwicklung Wissenschaftlichökonomischer Exzellenz (LOEWE Soft Control) for financial support of this work.

■ REFERENCES

(1) (a) White, S. R.; Sottos, N. R.; Geubelle, P. H.; Moore, J. S.; Kessler, M. R.; Sriram, S. R.; Brown, E. N.; Viswanathan, S. *Nature* **2001**, *409*, 794. (b) Chen, X.; Dam, M. A.; Ono, K.; Mal, A.; Shen, H.; Nutt, S. R.; Sheran, K.; Wudl, F. *Science* **2002**, *295*, 1698. (c) Zheludkevich, M. L.; Shchukin, D. G.; Yasakau, K. A.; Möhwald, H.; Ferreira, M. G. S. *Chem. Mater.* **2007**, *19*, 402. (d) Yuan, Y. C.; Yin, T.; Rong, M. Z.; Zhang, M. Q. *Express Polym. Lett.* **2008**, *2*, 238. (e) Cordier, P.; Tournilhac, F.; Soulié-Ziakovic, C.; Leibler, L. *Nature* **2008**, *451*, 977. (f) Cho, S. H.; White, S. R.; Braun, P. V. *Adv. Mater.* **2009**, *21*, 645. (g) Hager, M. D.; Greil, P.; Leyens, C.; van der Zwaag, S.; Schubert, U. S. *Adv. Mater.* **2010**, *22*, 5424.

(2) (a) Yoon, J. A.; Kamada, J.; Koynov, K.; Mohin, J.; Nicolaÿ, R.; Zhang, Y. Z.; Balazs, A. C.; Kowalewski, T.; Matyjaszewski, K. *Macromolecules* **2012**, *45*, 142. (b) Nakahata, M.; Takashima, Y.; Yamaguchi, H.; Harada, A. *Nat. Commun.* **2011**, *2*, 511. (c) Deng, G.; Li, F.; Yu, H.; Liu, F.; Liu, C.; Sun, W.; Jiang, H.; Chen, Y. *ACS Macro Lett.* **2012**, *1*, 275. (d) Yan, Q.; Feng, A.; Zhang, H.; Yin, Y.; Yuan. *J. Polym. Chem.* **2013**, *4*, 1216.

(3) Ma, Y. J.; Dong, W.-F.; Hempenius, M A.; Möhwald, H.; Vancso, G. J. *Nat. Mater.* **2006**, *5*, 724.

(4) (a) Wen, H.; Dong, C.; Dong, H.; Shen, A.; Xia, W.; Cai, X.; Song, Y.; Li, X.; Li, Y.; Shi, D. *Small* **2012**, *8*, 760. (b) Luo, Z.; Cai, K.; Hu, Y.; Zhao, L.; Liu, P.; Duan, L.; Yan, W. *Angew. Chem., Int. Ed.* **2011**, *123*, 666. (c) Cho, H.; Bae, J.; Garripelli, V. K.; Anderson, J. M.; Jun, H.-W.; Jo, S. *Chem. Commun.* **2012**, *48*, 6043. (d) de Gracia Lux, C.; Joshi-Barr, S.; Nguyen, T.; Mahmoud, E.; Schopf, E.; Fomina, N.; Almutairi, A. *J. Am. Chem. Soc.* **2012**, *134*, 15758. (e) Staff, R. H.; Gallei, M.; Mazurowski, M.; Rehahn, M.; Berger, R.; Landfester, K.; Crespy, D. *ACS Nano* **2012**, *6*, 9042.

(5) (a) Lallana, E.; Tirelli, N. *Macromol. Chem. Phys.* **2013**, *214*, 143. (b) Gracia, R.; Mecerreyes, D. *Polym. Chem.* **2013**, *4*, 2206.

(6) MacDiarmid, A. G. *Angew. Chem., Int. Ed.* **2001**, *40*, 2581.
(7) Abidian, M. R.; Kim, D. H.; Martin, D. C. *Adv. Mater.* **2006**, *18*, 405.
(8) Baughmann, R. H. *Synth. Met.* **1996**, *78*, 339.
(9) Baker, C. O.; Shedd, B.; Innis, P. C.; Whitten, P. G.; Spinks, G. M.; Wallace, G. G.; Kaner, R. B. *Adv. Mater.* **2008**, *20*, 155.
(10) Molberg, M.; Crespy, D.; Rupper, P.; Nuesch, F.; Manson, J. A. E.; Lowe, C.; Opris, D. M. *Adv. Funct. Mater.* **2010**, *20*, 3280.
(11) Tseng, R. J.; Haunag, J.; Ouyang, J.; Kaner, R. B.; Yang, Y. *Nano Lett.* **2005**, *5*, 1077.
(12) Gustafsson, G.; Cao, Y.; Treacy, G. M.; Klavetter, F.; Colaneri, N.; Heeger, A. J. *Nature* **1992**, *357*, 477.
(13) McQuade, D. T.; Pullen, A. E.; Swager, T. M. *Chem. Rev.* **2000**, *100*, 2537.
(14) Wang, L.-X.; Li, X.-G.; Yang, Y.-L. *React. Funct. Polym.* **2001**, *47*, 125.
(15) Bhadra, S.; Khastgir, D.; Singha, N. K.; Lee, J. H. *Prog. Polym. Sci.* **2009**, *34*, 783.
(16) (a) Barisci, J. N.; Lewis, T. W.; Spinks, G. M.; Too, C. O.; Wallace, G. G. *J. Intell. Mater. Syst. Struct.* **1998**, *9*, 723. (b) Rohwerder, M.; Michalik, A. *Electrochim. Acta* **2007**, *53*, 1300. (c) Cecchetto, L.; Ambat, R.; Davenport, A. J.; Delabouglise, D.; Petit, J. P.; Neel, O. *Corros. Sci.* **2007**, *49*, 818. (d) Rohwerder, M.; Duc, L. M.; Michalik, A. *Electrochim. Acta* **2009**, *54*, 607. (e) Rohwerder, M.; Isik-Uppenkamp, S.; Amarnath, C. A. *Electrochim. Acta* **2011**, *56*, 1889.
(17) (a) Lascelles, S. F.; Armes, S. P. *Adv. Mater.* **1995**, *7*, 864. (b) Lascelles, S. F.; Armes, S. P. *J. Mater. Chem.* **1997**, *7*, 1339. (c) Mangeney, C.; Bousalem, S.; Connan, C.; Vaulay, M.-J.; Bernard, S.; Chehimi, M. M. *Langmuir* **2006**, *22*, 10163. (d) Niu, Z.; Zhang, Z.; Hu, Z.; Lu, Y.; Han, C. C. *Adv. Funct. Mater.* **2003**, *13*, 949. (e) Jackowska, K.; Biegunski, A. T.; Tagowska, M. *J. Solid State Electrochem.* **2008**, *12*, 437. (f) Li, C. Y.; Chiu, W. Y.; Don, T. M. *J. Polym. Sci., Polym. Chem.* **2007**, *45*, 3902. (g) Cho, S. H.; Kim, W. Y.; Jeong, G. K.; Lee, Y. S. *Colloids Surf. A* **2005**, *255*, 79.
(18) (a) Zhang, L.; Wan, M. *Adv. Funct. Mater.* **2003**, *13*, 815. (b) Wei, Z.; Wan, M. *Adv. Mater.* **2002**, *14*, 1314.
(19) Crespy, D.; Landfester, K. *Beilstein J. Org. Chem.* **2010**, *6*, 1132.
(20) Schaeffel, D.; Staff, R. H.; Butt, H. J.; Landfester, K.; Crespy, D.; Koynov, K. *Nano Lett.* **2012**, *12*, 6012.
(21) Crespy, D.; Landfester, K. *Soft Matter* **2011**, *7*, 11054.
(22) Herrmann, C.; Crespy, D.; Landfester, K. *Colloid Polym. Sci.* **2011**, *289*, 1111.
(23) Schwab, M. G.; Crespy, D.; Feng, X. L.; Landfester, K.; Müllen, K. *Macromol. Rapid Commun.* **2011**, *32*, 1798.
(24) (a) van den Dungen, E. T. A.; Klumperman, B. *J. Polym. Sci., Polym. Chem.* **2010**, *48*, 5215. (b) Ouyang, X. B.; Huang, X. Q.; Pan, Q. H.; Zuo, C. Q.; Huang, C.; Yang, X. L.; Zhao, Y. B. *J. Dent.* **2011**, *39*, 825. (c) Fickert, J.; Makowski, M.; Kappl, M.; Landfester, K.; Crespy, D. *Macromolecules* **2012**, *45*, 6324. (d) Fickert, J.; Rupper, P.; Graf, R.; Landfester, K.; Crespy, D. *J. Mater. Chem.* **2012**, *22*, 2286. (e) Zhao, Y.; Fickert, J.; Landfester, K.; Crespy, D. *Small* **2012**, *8*, 2954. (f) Fickert, J.; Wohnhaas, C.; Turshatov, A.; Landfester, K.; Crespy, D. *Macromolecules* **2013**, *46*, 573.
(25) (a) Marie, E.; Rothe, R.; Antonietti, M.; Landfester, K. *Macromolecules* **2003**, *36*, 3967. (b) Bhadra, S.; Singha, N. K.; Khastgir, D. *Synth. Met.* **2006**, *156*, 1148.
(26) Shchukin, D. G.; Köhler, K.; Möhwald, H. *J. Am. Chem. Soc.* **2006**, *128*, 4560.
(27) Blinova, N. V.; Stejskal, J.; Trchova, M.; Prokes, J.; Omastrova, M. *Eur. Polym. J.* **2007**, *43*, 2331.
(28) Jamal, R.; Abdiryim, T.; Ding, Y.; Nurulla, I. *J. Polym. Res.* **2008**, *15*, 75.
(29) Wang, X.; Ray, S.; Gizdavic-Nikolaidis, M.; Easteal, A. J. *J. Polym. Sci., Polym. Chem.* **2012**, *50*, 353.
(30) Kim, Y. H.; Foster, J.; Chiang, J.; Heeger, A. J. *Synth. Met.* **1989**, *29*, 285.
(31) Fatuch, J. C.; Soto-Oviedo, M. A.; Avellaneda, C. O.; Franco, M. F.; Romao, W.; De Paoli, M. -A.; Nogueira, A. F. *Synth. Met.* **2009**, *159*, 2348.
(32) Albuquerque, J. E.; Mattoso, L. H. C.; Balogh, D. T.; Faria, R. M.; Masters, J. G.; MacDiarmid, A. G. *Synth. Met.* **2000**, *113*, 19.
(33) Yu, Y.; Zhang, Y.; Jiang, Z.; Zhang, X. *Langmuir* **2009**, *25*, 10002.
(34) Kim, H.; Jeong, S.-M.; Park, J.-W. *J. Am. Chem. Soc.* **2011**, *133*, 5206.
(35) Inzelt, G.; Pineri, M.; Schultze, J. W.; Vorotyntsev, M. A. *Electrochim. Acta* **2000**, *45*, 2403.
(36) Schnitzler, D. C.; Meruvia, M. S.; Hümmelgen, I. A.; Zarbin, A. J. G. *Chem. Mater.* **2003**, *15*, 4658.
(37) Li, C. M.; Sun, C. Q.; Chen, W.; Pan, L. *Surf. Coat. Technol.* **2005**, *198*, 474.
(38) (a) Sherif, E.-S. M.; Es-Saheb, M.; El-Zatahry, A.; Kenawyand, E.-R.; Alkaraki, A. S. *Int. J. Electrochem. Sci.* **2012**, *7*, 6154. (b) Souza, S. *Surf. Coat. Technol.* **2007**, *201*, 7574. (c) Khelifa, F.; Druart, M.-E.; Habibi, Y.; Bénard, F.; Leclère, P.; Olivier, M.; Dubois, P. *Prog. Org. Coat.* **2013**, *76*, 900. (d) Pereira da Silva, J. E.; Cordoba de Torresi, S. I. R.; Torresi, M. *Prog. Org. Coat.* **2007**, *58*, 33. (e) Chougrani, K.; Boutevin, B.; David, G.; Seabrook, S.; Loubat, C. *J. Polym. Sci., Part A: Polym. Chem.* **2008**, *46*, 7972.